LANGMUIR

pubs.acs.org/Langmuir Article

Hydrolysis of Poly(fluoroacrylate) Thin Films Synthesized from the Vapor Phase

Simon Shindler and Rong Yang*



Cite This: Langmuir 2023, 39, 1215-1226



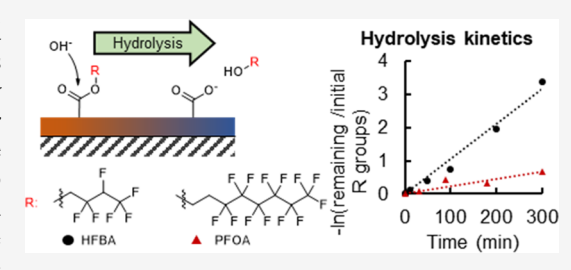
ACCESS

III Metrics & More

Article Recommendations

Supporting Information

ABSTRACT: The post-synthesis surface reaction of vapor-deposited polymer thin films is a promising technique in engineering heterogeneous surface chemistry. Because the existing research has neglected marginally reactive precursor films in preference of their highly reactive counterparts, our knowledge of kinetics and loss of film integrity during the reaction are limited. To address these limitations, we characterize hydrolysis of two fluoroacrylates, poly(1H,1H,2H,2H-perfluorooctyl acrylate) (pPFOA) and poly(2,2,3,4,4,4-hexafluorobutyl acrylate) (pHFBA), with sodium hydroxide using X-ray photoelectron spectroscopy. Without crosslinking with di-



(ethylene glycol)divinyl ether (DEGDVE) and grafting with trichlorovinyl silane, the films degrade rapidly during hydrolysis. An $S_{\rm N}2$ mechanism describes hydrolysis well, with rate constants of 0.0029 ± 0.0004 and 0.011 ± 0.001 L mol $^{-1}s^{-1}$ at 30 °C for p(PFOA-co-DEGDVE) and p(HFBA-co-DEGDVE), respectively. Our detailed study of hydrolysis kinetics of marginally reactive fluoroacrylates demonstrates the full capability and limitations of the post-synthesis reaction. Importantly, copolymers are characterized using a density correction new to polymer chemical vapor deposition.

■ INTRODUCTION

Polymer coatings and thin films are frequently used to modify surface chemistry.^{1,2} Fluoroacrylic polymers often find applications for their low dielectric constant, low friction coefficient, low refractive index, low surface energy, low flammability, inertness to chemicals, and interesting repellency of both polar and non-polar liquids.³ They are often used as coatings to prevent weathering and other forms of aging. The two representative fluoroacrylates are poly(1H,1H,2H,2Hperfluorooctyl acrylate) (pPFOA) and poly(2,2,3,4,4,4-hexafluorobutyl acrylate) (pHFBA), which have both found applications as self-cleaning hydrophobic coatings.^{5,6} The base-catalyzed hydrolysis of these fluoroacrylates is of interest for three reasons. First, polymers with long perfluorinated side chains (like pPFOA) are unique for their low surface energy but can introduce bio-persistent, carcinogenic perfluorinated acids (PFAs) into the environment (notably eight-carbon PFAs). Therefore, understanding the hydrolysis of fluoroacrylates is important in estimating the environmental release of PFAs from polymeric sources. Second, the partial hydrolysis of fluoroacrylates may lead to novel amphiphilic surfaces, which have been useful in antifouling applications.8 Finally, hydrolysis of fluoroacrylic polymers has interesting applications in the fabrication of spatially non-uniform coatings. These applications are the primary motivation for our study and warrant a more in-depth discussion.

Techniques which enable in-plane surface chemistry nonuniformity (distinct from film non-uniformity normal to the surface) are a significant development in our ability to engineer surfaces. Due to their hydrophobicity, fluoropolymer thin films are difficult to synthesize using traditional methods, so this discussion of film surface chemistry non-uniformity will be limited to polymer chemical vapor deposition (CVD) techniques (in-depth discussion of polymer CVD will follow). The existing polymer CVD research focuses on three main applications of in-plane surface chemistry non-uniformity: Janus membranes, 9-12 templated (or patterned) surfaces, 13-15 and chemical gradients. 16-18 Janus membranes are valuable in applications such as membrane distillation, water collection in arid environments, breathable fabric for activewear, and wound dressings with improved blood barrier and wound protection properties. 19,20 Templating is used to produce patterns of two contrasting chemistries, which may be used for drug release, biosensors, and artificial skins. 13-15 Films with chemical gradients have been used to mimic in vivo cellular growth conditions. 16-18

Spatially selective reaction of thin films can be applied to any of these applications of spatially non-uniform coatings as a post-synthesis modification, but research has been limited. In the solution phase, post-synthesis modification is common and frequently performed to obtain chemistries which do not polymerize directly.²¹ Broadly, this paradigm extends into the

Received: November 2, 2022 Revised: December 25, 2022 Published: January 9, 2023





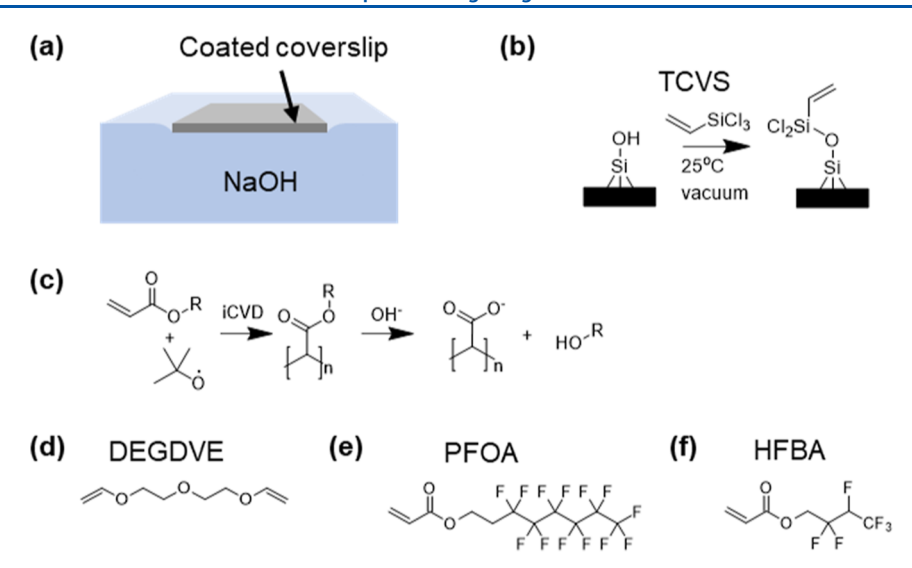


Figure 1. Reaction schema and chemical structures relevant to thin-film hydrolysis. (a) Schematic showing the working principle of using the surface reaction to react samples, (b) reaction scheme showing TCVS grafting, (c) reaction scheme showing polymerization, followed by hydrolysis, (d) chemical structure of DEGDVE, (e) chemical structure of PFOA, and (f) chemical structure of HFBA.

heterogeneous (surface) reaction of solid polymers in which unique surface chemistries are generated and bulk properties are decoupled from surface properties. Because these applications are often unconcerned with the surface chemistry of the precursor polymer, polymer thin-film research remains limited to highly reactive precursors. A common example of this is the decoration of a surface with large biomolecules such as enzymes (often by nucleophilic substitution of reactive esters).

There are two main gaps in our understanding of the postdeposition thin-film reaction. First, the established techniques, while powerful, treat the precursor-reactive polymer chemistry as sacrificial, indicating that the primary design constraint for the choice of precursor is to maximize the reactivity. When patterning a surface, or creating a Janus material, the precursor chemistry is left behind following modification, so unless extra steps are added to change the precursor chemistry, the requirement that one uses a highly reactive precursor limits the range of possible surfaces we can create. By exploring hydrolysis of marginally reactive fluoroacrylates, we can expand the domain of precursor chemistries and, by extension, expand the domain of potential non-uniform surface chemistries obtained by the post-synthesis reaction. Second, within the field of polymer CVD, there exist numerous examples of the post-deposition reaction; however, because the existing literature is made up primarily of application-oriented studies of highly reactive films, the kinetics of these reactions remains poorly understood. 12,14,16,17,25-44 Overall, the precursor surface chemistry has been rarely considered when using the postdeposition reaction of polymer thin films to obtain nonuniform surface chemistry.1

Investigation of pHFBA and pPFOA thin-film hydrolysis is an excellent place to start to understand the limitations of the post-synthesis reaction. Because the primary utility of fluoropolymers is their passivating properties, they present a difficulty for the post-deposition reaction. Because of the current lack of research in the post-synthesis reaction of marginally reactive polymers, further research is required to use the post-synthesis reaction on passivating or hydrophobic precursors.

Solution-phase processing methods such as spin coating and dip coating are effective in many applications; unfortunately, coating defects in fluoropolymer films are common due to the dewetting caused by low surface energy,⁴⁵ so it is challenging to produce uniform fluoropolymer thin films. 46,47 Polymer CVD is a powerful method of synthesizing hydrophobic polymer films and has demonstrated excellent conformality on micro- and nanostructures. 46,47 Polymer CVD eliminates the use of solvents, so post-polymerization extraction or solvent removal is no longer required, reducing the environmental impact of solvents and improving the cost-effectiveness of the synthesis. Because polymer CVD occurs in the vapor phase, there are no solubility restrictions on the chemistry of the precursor polymers, yielding uniform coatings with even the most hydrophobic monomers. 46,47 While polymer CVD refers to a range of techniques including plasma-enhanced CVD,⁵ parylene CVD, 16 and oxidative CVD, 48 this investigation focuses on initiated CVD (iCVD)⁴⁹ due to its compatibility with acrylate chemistry, 50 including PFOA and HFBA.

To better understand the limits of surface reactions of thin films, we hydrolyze crosslinked and uncrosslinked pHFBA and pPFOA with sodium hydroxide (NaOH) to determine the reaction kinetics and the effect of crosslinking on film stability during hydrolysis. Di(ethylene glycol)divinyl ether (DEGDVE) (Figure 1d) was chosen as a crosslinker because it is reasonably inert to NaOH⁵¹ and hydrophilic, enhancing the difference in hydrophilicity following hydrolysis. Grafting with trichlorovinyl silane (TCVS) (Figure 1b) is frequently used to prevent film delamination and is used to stabilize films during hydrolysis. We choose base-catalyzed hydrolysis for three reasons. The -OH ion is small and is therefore an effective nucleophile for penetrating into the fluoropolymer. While hydrolysis will always yield carboxylic acids, it is made significantly more versatile by the fact that the carboxylic acid moiety can readily undergo secondary functionalization reactions. 52-54 Base-catalyzed hydrolysis is favored over acidcatalyzed hydrolysis because siloxane bonds and ethers in the grafting agent and crosslinker are more easily hydrolyzed in acidic environments.

We aim to determine the conditions under which aqueous hydrolysis of uncrosslinked fluoroacrylates removes the

Table 1. Deposition Conditions

	fluoroacrylate fraction	$P_{\text{tot}} $ (Torr)	$T_{ ext{stage}} \ (^{\circ}\text{C})$	F_{TBPO} (sccm)	$F_{ m DEGDVE} \ m (sccm)$	F_{HFBA} (sccm)	$F_{ m PFOA} (m sccm)$	$F_{\rm Ar}$ (sccm)	thickness (nm)	deposition rate (nm/min)
p(HFBA-co-DEGDVE)	0.46 ± 0.03	0.1	10	0.10	0.05	0.48			189.6	7.0
p(PFOA-co-DEGDVE)	0.87 ± 0.02	0.1	15	0.14	0.08		0.1		153.4	1.3
pHFBA	1	0.5	30	1.06		1.08			~150	
pPFOA	1	0.05	10	0.06			0.30		360.3	45.0
pHFBA	1	1.1	30	0.99		1.99		0.99	459.1	

polymer film, which is useful for understanding the limitation of the film reaction and conditions under which the film might be deliberately removed (for purposes such as etching). We then aim to characterize the reaction kinetics of pPFOA and pHFBA to enable the conversion of a low surface energy hydrophobic fluorinated surface to a hydrophilic surface with poly(acrylic acid) functionality. By studying iCVD thin films, we are able to monitor thin-film-specific degradation processes (such as film delamination) and clearly observe degradation processes which might be obscured if working with the bulk polymer (such as film pitting) while retaining the ability to accurately quantify the reaction kinetics.

MATERIALS AND METHODS

Materials. DEGDVE (99%, from Aldrich) (Figure 1d), 1H,1H,2H,2H-perfluorooctyl acrylate (PFOA) (97%, from Oakwood Chemical) (Figure 1e), and 2,2,3,4,4,4-hexafluorobutyl acrylate (HFBA) (95%, from Aldrich) (Figure 1f) were used as monomers during deposition. Di-tert-butyl peroxide (TBPO) (98%, from Aldrich) was used as an initiator. All chemicals were used without purification. Deposition was performed on polished p/boron-doped silicon wafers as a reference to monitor the thickness with an in situ interferometer and for ellipsometry and Fourier transform infrared spectroscopy (FTIR) characterization. Deposition of samples that were destined to be hydrolyzed was performed on 2.2 cm square glass coverslips (Fisherbrand). Glass coverslips were used for hydrolysis experiments because the reaction of silicon wafer with NaOH interfered with the analysis, while the reaction of NaOH with glass was too slow to impact our experiment.

Compressed oxygen for plasma cleaning and ultrahigh-purity compressed argon as an iCVD patch gas were obtained from Airgas. TCVS (97%, from Aldrich Chemical) was used for grafting of the polymer film to the substrate.

NaOH solution was prepared in a volumetric flask with Milli-Q water from a Q-POD Biopak polisher (cat. no. CDUFBI001), and NaOH pellets (99%) were used without purification from Sigma-Aldrich. Milli-Q water was also used for sample cleaning following hydrolysis.

iCVD Deposition. Vapor deposition of polymer thin films occurred in a custom-built iCVD reactor. The pressure in the reactor was monitored with an MKS Baratron capacitance manometer model 626C and was controlled with an MKS throttle valve (model no. 253B) at the outlet of the reactor. TBPO was used as an initiator, and the flow rate of vapor was controlled using an MKS mass flow controller type 1159B. The flow of each monomer was controlled using a needle valve. All monomers and TBPO vapors were introduced to the reactor from the liquid contained in the glass vials attached to the reactor. To ensure sufficient volatility, DEGDVE and PFOA were heated at 80 and 60 °C, respectively. HFBA and TBPO were not heated. The temperature of the reactor filament array was monitored with a k-type thermocouple during the deposition (220 °C during all depositions). The leak rate of the reactor was measured as less than 0.05 sccm before each deposition. The reactor stage was cooled using an Accel 500 LT recirculating chiller (Fisher Scientific). The filament was resistively heated using a BK Precision DC power supply.

Gas flow rates and leak rate were measured by closing the throttle valve to the reactor and measuring the linear increase in pressure as gas flowed into the chamber. The increase in pressure was related to the flow using the volume of the reactor and the ideal gas law (equation S1 in the Supporting Information). The average and standard deviation of three measurements are reported. Monomer total pressure and monomer saturation pressure were calculated according to equations S.2—S.4 in the Supporting Information.

Copolymer p(HFBA-co-DEGDVE) was deposited on glass slides and silicon wafers. Both grafted and ungrafted samples were prepared in the same deposition for consistency of results. A homopolymer p(HFBA) film grafted with TCVS was deposited on glass slides and silicon wafers. An ungrafted homopolymer p(HFBA) film was deposited on silicon wafer to be used solely as a reference sample in FTIR composition analysis. The grafted homopolymer p(PFOA) was deposited on silicon wafers and glass slides for hydrolysis and as a reference sample in FTIR analysis. The grafted and ungrafted p(PFOA-co-DEGDVE) was deposited on glass slides and silicon wafers. See Table 1 for deposition conditions corresponding to each run.

Grafting. The samples were cleaned in oxygen plasma using a PDC-001-HP plasma cleaner with a PDC-FMG PlasmaFlo from Harrick plasma on the high setting for 2 min. The samples were then transferred directly to a chamber with 0.5 mL of TCVS, and air was evacuated using house vacuum. The samples were removed after 2 min and moved directly to the iCVD reactor.

Hydrolysis. Grafted pHFBA, pPFOA, and grafted and ungrafted p(HFBA-co-DEGDVE) and p(PFOA-co-DEGDVE) samples deposited on glass slides were allowed to float on roughly 20 mL of NaOH in a beaker and stirred at 200 rpm on a hotplate. We assumed a constant NaOH concentration over the course of the reaction based on the quantity of NaOH used, as there are $\sim 10^{-2}$ mol of -OH ions in the 20 mL 1 M NaOH solution used for the reaction, while we estimate $\sim 10^{-7}$ mol of functional groups in the polymer film. Even so, fresh NaOH was used between samples. The temperature of the hotplate was controlled at 30 °C for all reactions and temperature equilibrated for 30 min prior to the reaction. 30 $^{\circ}\text{C}$ was chosen since it was the lowest temperature on the hotplate and therefore the lowest temperature we could reliably control since room temperature might fluctuate from day to day. Evaporation was prevented by sealing the beaker with a parafilm. At the end of the reaction, the samples were removed, quickly dried with nitrogen gas to prevent further reaction, rinsed thoroughly with Milli-Q water, and dried again with nitrogen.

Characterization. Infrared spectra were collected using a Nicolet iS50 FTIR spectrophotometer in the transmission mode at a resolution of 4 cm⁻¹ with a DGTS detector from 600 to 4000 cm⁻¹. A variable angle grazing angle attenuated total reflectance attachment with a germanium crystal was used to collect monomer spectra by placing a few drops of monomer on the crystal. Omnic software was used for analysis and peak integration. Omnic was also used for baseline correction, and a comparison between uncorrected and corrected spectra can be found for pHFBA in Figure S8 in the Supporting Information.

Film thickness was characterized using a JA Woolam alpha-SE spectroscopic ellipsometer with data taken at 65, 70, and 75° . The data was fitted using Complete EASE 6 software version 6.51. Polymer films were modeled as Cauchy films.

Dynamic contact angle was characterized using the sessile drop method with a Ramé-Hart goniometer with a 150 W fiber optic illuminator. Water was pumped out until a sufficiently accurate advancing contact angle was observed, and then water was pumped

back to measure the receding contact angle. Measurements over \sim 20 datapoints were averaged, and standard deviation was reported as a measurement error.

Optical microscopic images were captured with a VHX-970F digital microscope from Keyence in the reflectance mode. Depending on the scale desired, either 500× magnification or 50× magnification was used

X-ray photoelectron spectroscopy (XPS) survey scans were collected from samples using a ScientaOmicron ESCA 2SR XPS. The pass energy was 150 eV, and the filament voltage was 10 kV with a step size of 1 eV. A flood gun was used for sample neutralization. Angle-resolved XPS (AR-XPS) was performed by tilting the sample relative to the detector to vary the emission angle. The sample was tilted at 0° (standard orientation), 20°, 40°, and 50°. Data analysis and peak integration were performed using CasaXPS software. The inelastic mean free path (IMFP), used to estimate the sampling depth, was calculated using QUASES-IMFP-TPP2M Ver. 3.0 software. ⁵⁵

RESULTS AND DISCUSSION

iCVD Synthesis and FTIR Analysis. Thin films of pPFOA, p(PFOA-co-DEGDVE), pHFBA, and p(HFBA-co-DEGDVE) were synthesized using the iCVD technique, and the conditions are listed in Table 1. The thickness-normalized FTIR transmission spectra of the films were collected (Figure 2). DEGDVE, PFOA, and HFBA monomer spectra were collected using FTIR with attenuated total reflectance (FTIR-ATR), so the absorbance of peaks at a higher wavenumber is reduced. ⁵⁶

Peaks belonging to the acrylic ester functionality (discussed below) can be identified in the monomers, homopolymers, and copolymers of HFBA and PFOA. In general, the acrylate peaks are larger in the pHFBA spectra than in the pPFOA spectra, in part because the number density of the acrylate moiety per unit polymer volume is less for the bulkier PFOA monomer. The peak at $\sim 1730~{\rm cm}^{-1}$ (dark blue \odot) is due to C=O stretching in the acrylate. The peak at 1280 cm⁻¹ (red \bigodot) is due to asymmetric stretching of the acrylate. The peak at 1150 cm⁻¹ (orange \bigodot) is due to the C-O stretching of the acrylate. The peak at 1100 cm⁻¹ (yellow \bigodot) is due to either ester asymmetric stretching or the SiO₂ substrate and is difficult to decouple. The peak at 840 cm⁻¹ (green \bigodot) is due to the C-C bond of the acrylic ester.

Peaks belonging to vinyl groups in both the acrylate and vinyl ether are present in the monomer spectra but are not present in the corresponding polymer spectra. Most notably, the peaks around $1625 \, \mathrm{cm}^{-1}$ (purple \triangle) in monomer spectra are due to C=C stretching, and their absence in polymer spectra indicates that full polymerization has occurred for all films. Furthermore, it shows that there are very few, if any, labile vinyl bonds in the crosslinked spectra, indicating that DEGDVE is highly reactive with the acrylic monomers. The peaks around $1400 \, \mathrm{cm}^{-1}$ (agreen trapezoid) are due to alkane CH₂ scissoring and CH bending. The peak at 950 cm⁻¹ (light blue \bigcirc) is due to acrylate C=C. The peak at 800 cm⁻¹ (blue \bigcirc) is due to the out-of-plane CH₂ vibration of the vinyl bond.

Peaks belonging to fluorocarbon bond vibrations can be identified in all fluoropolymer spectra. The peaks at 1230 and 1200 cm⁻¹ (•black L) are due to the carbon fluorine bond in the fluorocarbon. Peaks around 700 cm⁻¹ present in fluorine-containing spectra (but not labeled) are due to the C–F deformation broadly.

Peaks in the DEGDVE monomer spectrum are not found prominently in the p(PFOA-co-DEGDVE) or p(HFBA-co-DEGDVE) spectra since the peaks which do not overlap with

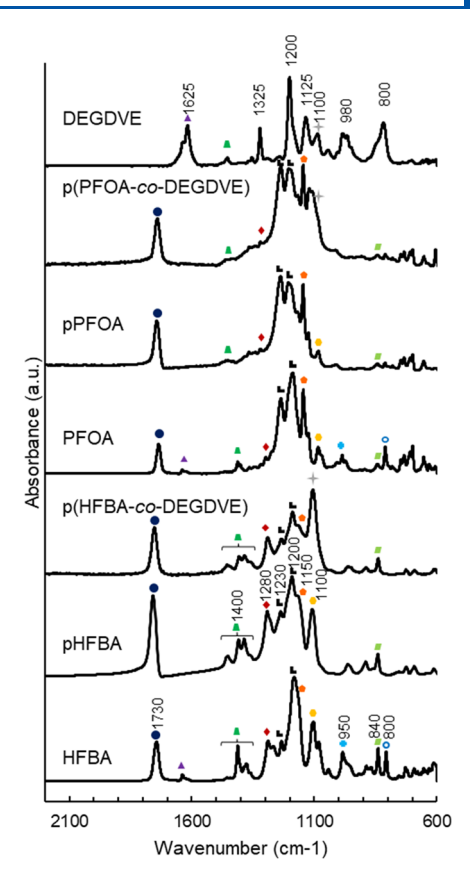


Figure 2. FTIR spectra of monomers and polymers. FTIR spectra of DEGDVE monomer, p(PFOA-co-DEGDVE), pPFOA, PFOA monomer, p(HFBA-co-DEGDVE), pHFBA, and HFBA monomer. Polymer spectra were collected in the transmission mode and were normalized by their film thickness. Monomer spectra were collected using FTIR-ATR and were normalized to be of the same general scale as they cannot be used for quantification.

acrylate or fluorocarbon peaks are associated with the vinyl ether and disappear on polymerization. The other characteristic DEGDVE peaks appear at around 1100 cm $^{-1}$ in the crosslinked films. The peak at 1325 cm $^{-1}$ is due to the =CH rocking vibration of the vinyl ether. The peak at 1200 cm $^{-1}$ is due to the asymmetric stretching of C-O-C stretching. The peaks at 1125 and 1100 cm $^{-1}$ (+grey +) are due to the stretching of the central ether of DEGDVE. The peak at 980 cm $^{-1}$ is due to vinyl ether wagging, and the peak at 800 cm $^{-1}$ is due to vinyl ether symmetric C-O-C stretching.

Composition Analysis Using FTIR with Ellipsometry. The composition of thin films can be determined using FTIR of the "bulk" polymer film. FTIR in the transmission mode is a more effective method of quantification than XPS since it samples the whole film and it is not biased by surface non-uniformities. Equation 1 gives the mole fraction of fluoroacrylate (HFBA or PFOA moiety) $x_{\rm m}$ in the crosslinked film and is based on the assumption that the Lorenz–Lorentz equation can be used to relate the film refractive index to the film density and that Beer's law relates the absorption of a peak in FTIR to the concentration of the associated moiety in the film. The Lorentz–Lorenz equation relies on the principle of the molar refraction, which is a measure of the total polarizability of a mole of the substance. Derivation of eq 1 can be found in the Supporting Information.

Table 2	Compositional	and Density	Data for	Homonolymer	and	Crosslinked Films
Table 2.	Compositional	and Density	Data IUI	TIOHIODOIVHEL	anu	CIUSSIIIIKCU I IIIIIS

	pHFBA	p(HFBA-co-DEGDVE)	pPFOA	p(PFOA-co-DEGDVE)
A (a.u.)	3.11	0.733	1.39	0.572
b (nm)	459.09 ± 0.10	189.59 ± 0.17	357.45 ± 0.11	153.38 ± 0.175
$Mr_{\mathrm{D_m}}(\mathrm{cm}^3 \mathrm{mol}^{-1})$	33.98	33.98	52.452	52.452
$Mr_{\mathrm{D}_{\mathrm{DEGDVE}}}(\mathrm{cm}^3 \mathrm{\ mol}^{-1})$		39.67		39.673
$n_{ m D}$	1.394 ± 0.004	1.567 ± 0.046	1.364 ± 0.001	1.392 ± 0.007
$ ho~({ m g~cm^{-3}})$	1.662 ± 0.015	1.71 ± 0.15	1.776 ± 0.004	1.801 ± 0.048
$x_{ m m}$	1	0.456 ± 0.033	1	0.87 ± 0.02

$$x_{\rm m} = \frac{Mr_{\rm D_{\rm DEGDVE}}}{Mr_{\rm D_{\rm m}} \frac{A_{\rm h}b_{\rm c}(n_{\rm D,h}^2 + 2)(n_{\rm D,c}^2 - 1)}{A_{\rm c}b_{\rm h}(n_{\rm D,h}^2 - 1)(n_{\rm D,c}^2 + 2)} + (Mr_{\rm D_{\rm DEGDVE}} - Mr_{\rm D_{\rm m}})}$$
(1)

where $Mr_{\rm D_{\rm DEGDVE}}$ and $Mr_{\rm D_{\rm m}}$ are the molar refractions of the DEGDVE moiety and the fluoroacrylate moiety (either PFOA or HFBA), A is the absorbance of the carbonyl peak at 1730 cm⁻¹ in the FTIR spectrum, $n_{\rm D}$ is the refractive index, and b is the film thickness from ellipsometry. Subscript "h" indicates the property of the homopolymer film and subscript "c" indicates the property of the copolymer film. The densities of the films can be calculated using the same assumptions as in eq

$$\rho = \left(\frac{n_{\rm D}^2 - 1}{n_{\rm D}^2 + 2}\right) \frac{M_{\rm DEGDVE} + (M_{\rm m} - M_{\rm DEGDVE})x_{\rm m}}{Mr_{\rm D_{\rm DEGDVE}} + (Mr_{\rm D_m} - Mr_{\rm D_{\rm DEGDVE}})x_{\rm m}}$$
(2)

where M is the formula weight of the moiety in question. Subscript "m" refers to either PFOA or HFBA and subscript "DEGDVE" refers to DEGDVE. The unit of density is g cm⁻³. The molar refraction of each of the moieties is determined using the group contribution method.⁵⁸

The refractive index and thickness were determined using spectroscopic ellipsometry, and refractive index values were taken at a wavelength of 589 nm, as is standard. The results of the composition analysis are presented in Table 2.

Note that both crosslinked films are denser than their homopolymer counterparts. Without correcting for this, we would underestimate the quantity of the crosslinker. Because a group contribution method was used to determine the molar refraction, these results should be taken as approximations of the true value; however, there is precedent for using refractive index to characterize the density of the polymer systems. 57 The refractive index of commercially available pHFBA is 1.394, essentially identical to our data from ellipsometry (Table 2); however, the density is 1.519 g cm⁻³,59 indicating that the molar refractivity given by the group contribution method has overestimated density by 10%. It is reasonable to expect a similar overestimation for PFOA. Note that due to the deposition kinetics, we were forced to use different crosslinking densities for the two polymers, and we acknowledge that this is certainly not ideal for comparison of film properties. We were unable to decrease the crosslinking density in p(HFBA-co-DEGDVE) because reliable DEGDVE flow rates below 0.05 sccm could not be obtained. The remarkably high fraction of crosslinker is likely due to the alternating behavior between the vinyl ether and the HFBA, which is a well-documented tendency in fluoroacrylates.4 We were unable to increase the crosslinking density in p(PFOA-co-DEGDVE) since a higher partial pressure of DEGDVE would have caused condensation.

Role of Grafting and Crosslinking in Film Stability. The as-deposited pPFOA films were reacted with 1 M NaOH

at 30 °C for 40 min, and the pHFBA films were reacted with 0.5 M NaOH at 30 °C for 30 min. 30 °C was used for all hydrolysis experiments since it was the lowest temperature we could reliably control using the hotplate. The goal of this experiment was solely to illustrate degradation, so a lower concentration of NaOH was used for the hydrolysis of pHFBA films to slow degradation and enable clear characterization. Additionally, different reaction times are reported based on when degradation was most clearly observed. Micrographs of the films show apparent pitting (Figure 3a,b), indicating

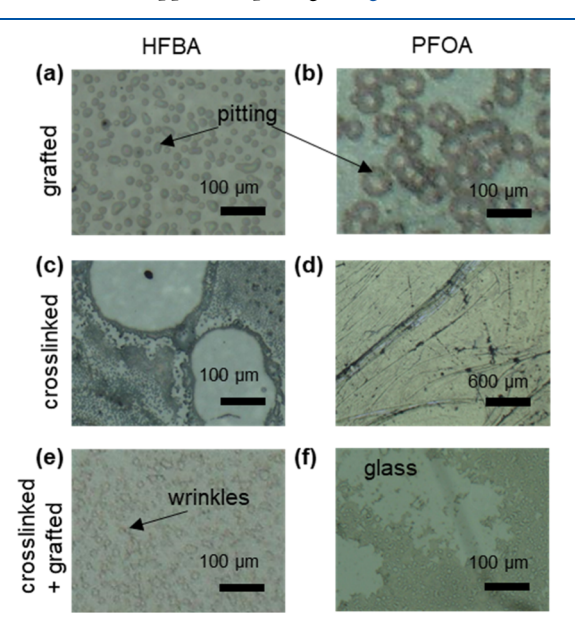


Figure 3. Optical micrographs of iCVD films treated with aqueous solutions of NaOH: (a) pHFBA film grafted with TCVS showing pitting after 30 min in 0.5 M NaOH, (b) pPFOA film grafted with TCVS showing pitting after 40 min in 1 M NaOH, (c) p(HFBA-co-DEGDVE) film (not grafted) showing delamination after 2 min in 1 M NaOH, (d) p(PFOA-co-DEGDVE) film (not grafted) showing delamination after 2 min in 1 M NaOH, (e) p(HFBA-co-DEGDVE) film grafted with TCVS showing wrinkling after 300 min in 1 M NaOH, and (f) p(PFOA-co-DEGDVE) film grafted with TCVS showing degradation after 300 min in 1 M NaOH.

gradual film disintegration during hydrolysis. Because the reaction product of homopolymer pPFOA and pHFBA is poly(acrylic acid), a water-soluble polymer, ⁶⁰ it is unsurprising that films of pPFOA and pHFBA would gradually disintegrate as they are converted to poly(acrylic acid). Based on this hypothesized mechanism of degradation, the only way to prevent degradation is by modifying the film in such a way to make the product insoluble, whereas different strengths of nucleophile or base should have little effect. The film degradation observed in uncrosslinked films made accurate

characterization of the surface hydrolysis reaction nearly impossible. Further investigation of the pitting and delamination in Figure 3 would be necessary to fully understand how these occur and develop over time; however, our interest lies instead with the root causes and mitigating measures of degradation. Crosslinking was used to prevent film dissolution. DEGDVE, a common crosslinker in iCVD,³¹ was used because it is hydrophilic, enabling us to see the maximum difference in hydrophilicity following hydrolysis, and is stable in NaOH at moderate temperatures.⁵¹

The ungrafted copolymers, p(PFOA-co-DEGDVE) and p(HFBA-co-DEGDVE), showed serious film delamination (Figure 3c,d) after only 2 min of exposure to 1 M NaOH, indicating that grafting was required to achieve a film capable of withstanding even small amounts of hydrolysis. Delamination is caused by insufficient van der Waals interactions between the film and the substrate and is generally solved by covalently bonding the film to the surface using a silane coupling agent. As such, all films used in reaction characterization were grafted to glass coverslips using TCVS.

Grafted and crosslinked p(PFOA-co-DEGDVE) and p-(HFBA-co-DEGDVE) were significantly more stable during hydrolysis in 1 M NaOH with both films showing good stability up to 300 min. After 300 min, however, p(HFBA-co-DEGDVE) films began to wrinkle (Figure 3e). This may be caused by hydrolysis of the siloxane bonds holding it to the surface, 61 or it may be caused by film swelling. At 300 min, p(PFOA-co-DEGDVE) films were observed to begin to degrade significantly (Figure 3f). XPS characterization was performed on less degraded portions of the film, which we know to be continuous based on the lack of silicon peaks. Discontinuous films show silicon peaks from the glass substrate (see Figure S2 in the Supporting Information). The p(PFOAco-DEGDVE) films contained a less crosslinker than p(HFBAco-DEGDVE), so it is unsurprising that they would degrade faster; however the apparent delamination indicates that hydrolysis of the siloxane bonds holding the film to the substrate is occurring and that better coupling methods must be developed if thin films are to be used in caustic environments for any length of time. Improving the resistance of coupling agents to hydrolysis is a broader problem in the field, with dipodal silanes representing a possible improvement.⁶²

The rapid destruction of uncrosslinked and ungrafted fluoroacrylate thin films indicates that NaOH is an effective method of film removal and could be used to remove hydrolysable films for etching or in the fabrication of Janus materials. These findings also inform the use of fluoroacrylates more generally as they indicate that hydrolysis of uncrosslinked fluoroacrylate bulk polymers is not localized to the top surface but instead causes degradation of the polymer. While this is relevant to any application of acrylates in potentially caustic environments, it is especially relevant to fluoroacrylates such as PFOA, which can introduce carcinogenic PFA into the environment through hydrolysis. While crosslinking reduces the solubility of hydrolyzed films, grafting appears to be necessary to prevent rapid delamination (Figure 3f). As such, grafted p(HFBA-co-DEGDVE) and p(PFOA-co-DEGDVE) films were synthesized for reaction kinetics analysis.

Hydrolysis Kinetics. Hydrolysis of crosslinked and grafted p(HFBA-co-DEGDVE) thin films with 45.6 \pm 3.3% HFBA and p(PFOA-co-DEGDVE) thin films with 87 \pm 2% PFOA was performed by floating coated glass slides on NaOH solution as

depicted in Figure 1a. XPS was used to characterize the conversion. The XPS data only describes the film up to the analysis depth, ⁶³ which has been estimated using the TPP-2M formula ⁵⁵ to be on the order of 10 nm. The XPS survey scans of unreacted films were compared with films reacted for 300 min in 1 M NaOH, showing a significant decrease in the prominence of the fluorine 1s peak in PFOA and an almost complete disappearance of the fluorine 1s peak in HFBA samples. This suggests an almost complete loss of fluorine within the XPS analysis depth (~10 nm) and an emergence of sodium carboxylate on the surface of the film (the unprotonated reaction product of hydrolysis) (Figure 4). As

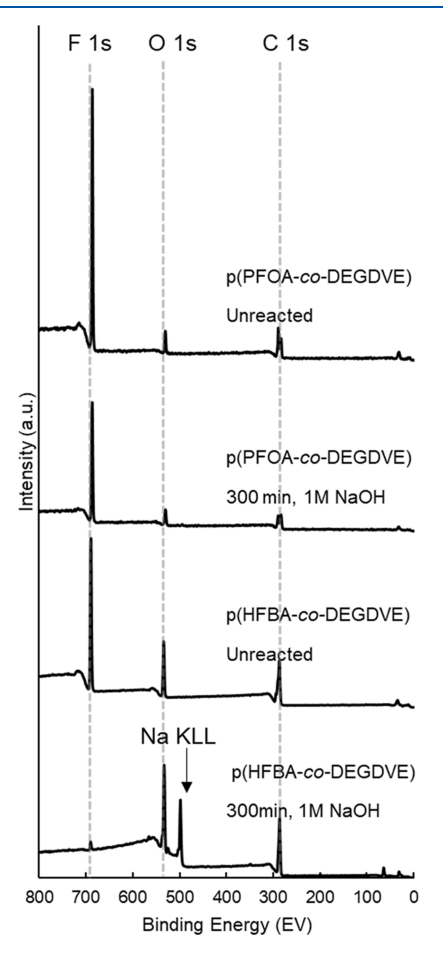


Figure 4. XPS data for unreacted p(HFBA-co-DEGDVE) and p(PFOA-co-DEGDVE) thin films and films reacted for 300 min in 1 M NaOH. Spectra corresponding to other time points are found in the Supporting Information (Figures S3–S7).

we have already stated, the absence of Si peaks confirms film continuity over the analysis area. All XPS survey scans used for kinetic analysis can be found in the Supporting Information.

The Damkohler number $Da = \frac{k n_m \hat{x}^2}{D}$ describes the relative effects of reaction and diffusion and can be used to characterize the degree to which concentrations measured with XPS are biased by diffusion-induced gradients. $\hat{x} = 10$ nm (the analysis depth) and D is the diffusion coefficient of NaOH in the polymer. The Damkohler number will be much less than 1 when the system is reaction-limited, so XPS characterization is unaffected by diffusion when $D \gg k n_{\rm m} \hat{x}^2 \sim 10^{-17} \ {\rm m}^2 \ {\rm s}^{-1}$. The measured diffusion coefficients of water in polymeric systems

are generally on the order of 10^{-13} m² s⁻¹,⁶⁴ so we do not expect compositional gradients resulting from reagent diffusion to exist within the XPS analysis depth.

Films of p(HFBA-co-DEGDVE) were reacted in two groups. In series (i), films were reacted in 1 M NaOH at 30 $^{\circ}$ C from 5 to 300 min to determine the kinetics with respect to surface functional groups. In series (ii), films were reacted at 30 $^{\circ}$ C for 50 min at NaOH concentrations ranging from 0.05 to 2 M to determine the kinetics with respect to NaOH concentration. We implicitly assume a constant NaOH concentration over the course of the reaction. Regarding this assumption, there are $\sim 10^{-2}$ mol of -OH ions in the 20 mL 1 M NaOH solution used for the reaction, while we estimate $\sim 10^{-7}$ mol of functional groups in the polymer film (based on polymer density). Even so, fresh NaOH was used between samples.

Films of p(PFOA-co-DEGDVE) were also reacted in two groups. Series (i) films were reacted in 1 M NaOH at 30 °C from 30 to 300 min to determine the kinetics with respect to surface functional groups, and series (ii) films were reacted at 30 °C for 180 min in 0.2–2 M NaOH to determine the kinetics with respect to NaOH concentration. The surface density of the HFBA or PFOA moiety in unreacted and reacted samples was quantified using XPS.

The fractional conversion X_m was calculated based on the fluorine atomic ratio (from XPS survey scans) using eq 3 (derived in the Supporting Information).

$$X_{\rm m} = \frac{x_{\rm F} - x_{\rm F}^0}{\left(\frac{\phi_{\rm m}}{\pi_{\rm m}} x_{\rm F} - 1\right) x_{\rm F}^0} \tag{3}$$

where $x_{\rm F}$ is the surface mole fraction of fluorine for a given sample as determined from the XPS survey scans and $x_{\rm F}^0$ is the surface mole fraction of fluorine for the unreacted sample, $\pi_{\rm m}$ is the number of fluorine atoms in the fluoroacrylate monomer (6 for HFBA and 13 for PFOA), and $\phi_{\rm m}$ is the number of carbon and fluorine atoms lost when a single fluoroacrylate moiety is hydrolyzed (10 for HFBA and 21 for PFOA). The surface mole fraction of fluorine was used in lieu of carbon or oxygen to avoid error introduced by adventitious carbon and oxygen. Adventitious carbon and oxygen are common in XPS, while fluorine contamination is not.

We hypothesize a general rate equation of arbitrary reaction order with respect to the concentration of NaOH c_{NaOH} and the surface number density of either HFBA or PFOA moiety n_{m} (eq 4).

$$-\frac{\mathrm{d}n_{\mathrm{m}}}{\mathrm{d}t} = kn_{\mathrm{m}}^{\alpha}c_{\mathrm{NaOH}}^{\beta} \tag{4}$$

where t is the reaction time, k is the rate constant, α is the reaction order with respect to the number density of HFBA or PFOA, and β is the reaction order with respect to NaOH. Solving eq 4 in terms of the fractional conversion of fluoroacrylate functionality $X_{\rm m} = \frac{n_{\rm m}^0 - n_{\rm m}}{n_{\rm m}^0}$ while keeping the concentration of NaOH constant gives eq 5.

$$-\ln(1 - X_{\rm m})$$

$$= \begin{cases} kc_{\rm NaOH}^{\beta}t & \alpha = 1\\ \frac{1}{1 - \alpha} \ln((\alpha - 1)kn_{\rm m}^{0\alpha - 1}c_{\rm NaOH}^{\beta}t + 1) & \alpha \neq 1 \end{cases}$$
(5)

To determine the reaction order with respect to the fluoroacrylate moiety, $-\ln(1-X_{\rm m})$ is plotted against time (Figure 5a), showing r^2 values of 0.99 for HFBA and 0.92 for

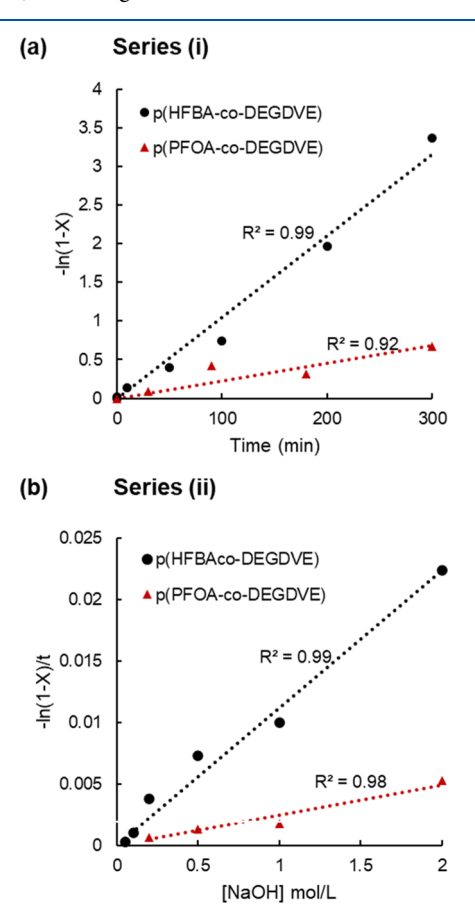


Figure 5. Data to determine the reaction kinetics. (a) Series (i), $-\ln(1-X_{\rm m})$ vs time for p(HFBA-co-DEGDVE) and p(PFOA-co-DEGDVE) thin films reacted in 1 M NaOH showing a first-order behavior with respect to the concentration of acrylate repeat units. (b) Series (ii), $-\ln(1-X_{\rm m})/t$ vs NaOH concentration for p(HFBA-co-DEGDVE) and p(PFOA-co-DEGDVE) thin films showing a first-order behavior with respect to NaOH concentration.

PFOA for a linear fit. From this data, we can conclude that a first-order approximation is valid for both hydrolysis of p(PFOA-co-DEGDVE) and p(HFBA-co-DEGDVE) up to a fractional conversion of 0.613 and 0.965, respectively. While a non-integer reaction order less than 1 provides a better fit to HFBA data, mechanistically, as a substitution reaction, we expect first-order behavior with respect to the concentration of the reactive surface moiety. As such, the deviation between the first-order and non-integer-order models is too small to justify and would be considered overfitting.

It is possible that this deviation is due to the chain reorientation within the XPS sampling volume. Fluorinated groups are preferentially excluded from the bulk, even in homo-fluoropolymers, 66 and the presence of carboxylic acid moieties and ethers (present in DEGDVE) likely increases the magnitude of this preferential orientation. As samples are placed under high vacuum for XPS analysis, the carboxylic acid moieties (capable of forming strong hydrogen bonds with each other) exclude the hydrophobic fluorinated side chains to the surface of the film, thereby increasing the concentration of fluorine within the XPS sampling area and making it appear as

though the reaction rate is less. This explanation is supported by AR-XPS, which shows higher density of fluorine at the sample surface (Table 3). This effect has been seen elsewhere as well.⁶⁶

Table 3. AR-XPS Mole Fractions for the p(HFBA-co-DEGDVE) Sample Reacted for 200 min in 1 M NaOH

emission angle (deg)	analysis depth, λ^a (nm)	$x_{\rm C}$	$x_{\rm O}$	$x_{ m F}$	$x_{ m Na}$
0	11.4	0.63	0.27	0.057	0.042
20	10.7	0.60	0.28	0.070	0.049
40	8.8	0.58	0.28	0.078	0.058
50	7.4	0.57	0.29	0.077	0.061

^aThe analysis depth λ of the X-ray used in XPS is reported as $\lambda = 3 \times IMFP \cos \theta$ (inelastic mean free path), where the IMFP is calculated from the non-relativistic TPP-2M formula using the QUASES-IMFP-TPP2M Ver. 3.0 software, ⁵⁵ and θ is the emission angle.

As we can see in Table 3, the mole fraction of carbon decreases as the angle-resolved measurement becomes more surface sensitive (larger angle) and that of oxygen, fluorine, and sodium increase, indicating that they are present in a higher proportion at the surface of the material. This is likely due to the aforementioned chain reorientation, and it indicates that the true fractional conversion of p(HFBA-co-DEGDVE) is slightly higher than the measured value.

Taking the reaction to be first order with respect to the fluoroacrylate moiety, we can simplify eq 5 by setting $\alpha = 1$. To determine the reaction order with respect to NaOH concentration, it is useful to re-express eqs 5 as 6.

$$-\frac{\ln(1-X_{\rm m})}{t} = kc_{\rm NaOH}^{\beta} \tag{6}$$

Equation 5 shows that for an arbitrary reaction order in NaOH concentration, $-\frac{\ln(1-X_m)}{t}$ follows a power law. Figure 5b shows a plot of $-\frac{\ln(1-X_m)}{t}$ versus NaOH concentration from series (ii), in which the NaOH concentration was varied from 0.05 to 2 M for HFBA and from 0.2 to 2 M for PFOA, showing a linear behavior with r^2 values of 0.99 for HFBA and 0.98 for PFOA, indicating that the reaction is first order for both polymers. Nucleophilic substitution reactions are categorized into S_N1 and S_N2 types. S_N1 reactions are unimolecular and depend on the concentration of the nucleophile, while S_N2 reactions are bimolecular and depend on both the concentration of the nucleophile and the substrate. Generally, S_N2 reactions are characterized by poor leaving groups and are limited by steric hinderance. Both the PFOA and HFBA side chains are poor leaving groups, so an S_N2 mechanism (first order in both NaOH and fluoroacrylate moiety) is reasonable for our system.

Having determined the reaction order with respect to NaOH concentration and functional group density, eq 5 is solved for the rate constant k and averaged over all reacted samples (n = 11 and 8 for HFBA and PFOA, respectively) to give 0.011 ± 0.001 L mol⁻¹ s⁻¹ for HFBA and 0.0029 ± 0.0004 L mol⁻¹ s⁻¹ for PFOA (mean \pm standard error). Base-catalyzed hydrolysis of acrylate and methacrylate monomers in an aqueous medium at 30 °C has previously been reported to have reaction rates ranging from ~ 0.05 to 0.5 L mol⁻¹ s⁻¹. Fartitioning of NaOH into the polymer matrix explains slower kinetics we observed. At the polymer/water interface, we

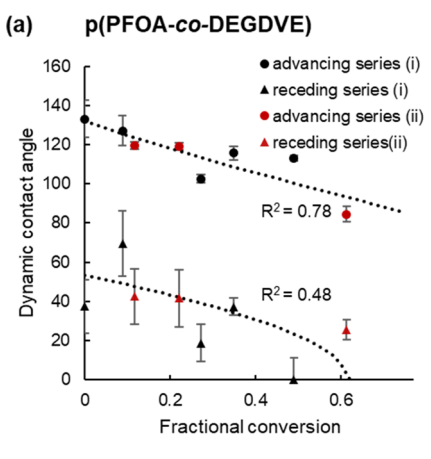
expect there to be a drop in the concentration of NaOH since it is more easily solvated in the liquid than in the polymer. This effect of partitioning should not change the order of reaction, but it will decrease the concentration of NaOH species available to react within the polymer relative to the bulk solution (where the concentration is known) and thereby reduce the measured reaction rate. Decoupling the partition coefficient from the reaction kinetics is out of the scope of this study. However, it should be noted that the reported rate constants are only valid for the crosslinking density studied, and changes in composition will likely change the kinetics. Solvation effects directly impacting the reaction kinetics⁶⁸ may be significant as well, but quantification of these is beyond the scope of this investigation.

The difference in reaction rate between p(PFOA-co-DEGDVE) and p(HFBA-co-DEGDVE) is also unsurprising and is likely due to both steric and inductive effects since HFBA is less bulky and fluorine atoms are located closer to the ester, thereby more effectively participating in electron withdrawing and making the HFBA functionality a better leaving group than PFOA.

Dynamic Contact Angle of Hydrolyzed Films. Dynamic water contact angles were measured on all p(HFBA-co-DEGDVE) and p(PFOA-co-DEGDVE) samples reacted with NaOH, showing a clear correlation between the dynamic contact angle and fractional conversion (Figure 6a,b). Note that the dynamic instead of static contact angles are reported because, for high hysteresis surfaces, it is likely that the measured static contact angles will deviate significantly from the Young's contact angle.⁶⁹ Therefore, it could be misleading to report a static contact angle for these samples. The overlap between data from series (i) and series (ii) indicates that two films reacted to the same final conversion using different NaOH concentrations likely have similar surface properties. Above ∼30% fractional conversion, water did not recede across the surface of p(HFBA-co-DEGDVE), so the receding contact angle is reported as 0°. The high hysteresis of both films is likely caused by roughness, viscoelasticity of the film, and chain reorientation (i.e., surface response to contact with water).⁷⁰ Chemical heterogeneity is cited as a common cause of dynamic contact angle hysteresis and is commonly modeled using the Cassie equation (eq 7); however in practice, the Cassie equation describes the minimum effect of heterogeneity on contact angle.⁷¹ Furthermore, the hydrolysis reaction likely changes the mechanical properties and roughness of the film, both of which will contribute to increasing contact angle hysteresis, which is not accounted for in the Cassie equation. The Cassie equation was fitted to the dynamic contact angle data of reacted p(HFBA-co-DEGDVE) and p(PFOA-co-DEGDVE) by performing a linear regression to the data on modified axes (see Figure S1). For p(PFOA-co-DEGDVE), the r^2 values were 0.48 and 0.78 for receding and advancing, respectively. For p(HFBA-co-DEGDVE), the r^2 was r^2 values were 0.65 and 0.93 for receding and advancing, respectively. The dotted lines in Figure 6 indicate the Cassie equation generated by the aforementioned curve fits of eq 7.

$$\cos \theta = f \cos \theta_1 + (1 - f) \cos \theta_2 \tag{7}$$

where f is the area fraction of the surface covered with chemistry 1. θ_1 and θ_2 then refer to the contact angle on a surface covered with chemistry 1 and 2, respectively. These were treated as fitting parameters. The fractional conversion



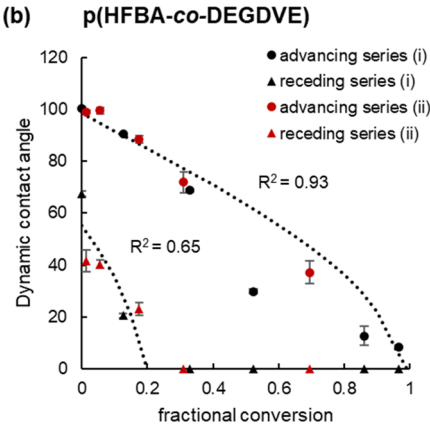


Figure 6. Dynamic contact angle data for hydrolyzed p(HFBA-co-DEGDVE) and p(PFOA-co-DEGDVE). Dynamic contact angle of (a) p(PFOA-co-DEGDVE) and (b) p(HFBA-co-DEGDVE) films reacted with aqueous NaOH vs fractional conversion. Series (i) refers to the time series data and series (ii) refers to the concentration series data. The black dotted lines are curve fits of the Cassie equation.

 $X_{\rm m}$ was assumed to be equal to the fractional surface coverage f

The poor fit for p(PFOA-co-DEGDVE) can be explained by random variation between samples; however, there appears to be a systematic overprediction of the advancing contact angle of p(HFBA-co-DEGDVE) at high conversion. We believe that this overprediction is related to the apparent mobility of the fluorine side chain suggested by AR-XPS. Under the high vacuum of XPS analysis, the fluorine side chains will preferentially cluster at the surface. When in contact with water during the dynamic contact angle measurement, they will reorient away from the surface. Reorientation of fluorine side chains away from the surface would effectively increase the fractional surface coverage of the hydrolyzed polymer relative to the measured fractional conversion resulting in the observed overprediction of the Cassie equation. Correcting for side chain mobility is outside the scope of this investigation.

CONCLUSIONS

Our work has characterized the hydrolysis reaction of p(PFOA-co-DEGDVE) and p(HFBA-co-DEGDVE) hydrolysis with NaOH, which can enable the fabrication of Janus or patterned chemical surface heterogeneity using marginally reactive precursor films by the post-synthesis surface reaction. Our kinetic data can be used to quantify the release of perfluorinated alcohols (which degrade to form PFAs) from

polymeric sources via hydrolysis. Such quantification is necessary to understand the impact of using polymers which can release these potentially toxic long-chain PFAs in the environment. Ellipsometric and FTIR data were used to determine the thin-film composition using a novel method which combines the Lorentz–Lorenz equation with Beer's law and demonstrates that when homopolymer and copolymer films have significant density differences, only using FTIR to characterize polymer composition causes errors.

By observing degradation of pHFBA and pPFOA, we show that modification of surface chemistry using the hydrolysis method requires both crosslinking and grafting. We have determined the rate equation for p(HFBA-co-DEGDVE) and p(PFOA-co-DEGDVE) hydrolysis with NaOH, showing both reactions to be well described by an $\rm S_{N}2$ -type model, which is first order in both the concentration of NaOH and the concentration of reactive moieties on the surface and second order overall. They have rate constants at 30 $^{\circ}\rm{C}$ of 0.011 \pm 0.001 L mol $^{-1}$ s $^{-1}$ for HFBA and 0.0029 \pm 0.0004 L mol $^{-1}$ s $^{-1}$ for PFOA. The more rapid reaction of HFBA can be explained by steric and inductive effects. AR-XPS performed on samples at high conversion shows densification of fluorine at the surface of the film caused by migration of the hydrophobic fluorinated side chains to the surface of the film once it is exposed to air.

The dynamic contact angle performed on the hydrolyzed samples shows that the wetting properties are strongly correlated with the fractional conversion. Furthermore, the absence of a significant change in contact angle hysteresis indicates that hydrolysis results in a homogeneous distribution of reacted moieties (under the assumption that roughness does not change significantly during hydrolysis). This indicates that partial hydrolysis of fluorinated films like those studied here may yield high-quality amphiphilic surfaces, which are useful for antifouling applications.⁸

In future research, hydrolysis followed by ammonolysis could enable the fabrication of diverse surface chemistries, including zwitterionic films. 52,72 Because $\rm S_{N}2$ reaction kinetics are often determined by sterics, we expect that the kinetics of nucleophilic amine substitutions onto hydrolyzed surfaces would be significantly more rapid than on the native fluoroacrylate. We would suggest further investigation into whether film removal of acrylates by NaOH can be used effectively as an etching method in film patterning or efficient fabrication of Janus materials. We would also suggest further investigation of the role that changing crosslinking density has in determining the reaction kinetics.

ASSOCIATED CONTENT

Supporting Information

The Supporting Information is available free of charge at https://pubs.acs.org/doi/10.1021/acs.langmuir.2c03005.

Derivations of equations used to calculate the flow rate measurements in the iCVD reactor, derivation of equations used to calculate the saturation pressure and partial pressure of the monomers, derivation of equations to calculate the fractional conversion from XPS data, derivation of kinetic equations to determine the reaction mechanism, derivation of equations used to determine the composition from Beer's law and the Lorentz—Lorenz equation, plots showing curve fitting of dynamic contact angle to the Cassie equation, XPS raw data for the concentration and time series for both

p(PFOA-co-DEGDVE) and p(HFBA-co-DEGDVE), and raw XPS data of a partially dissolved film (PDF)

AUTHOR INFORMATION

Corresponding Author

Rong Yang — Robert Frederick Smith School of Chemical & Biomolecular Engineering, Cornell University, Ithaca, New York 14853, United States; orcid.org/0000-0001-6427-026X; Email: ryang@cornell.edu

Author

Simon Shindler — Robert Frederick Smith School of Chemical & Biomolecular Engineering, Cornell University, Ithaca, New York 14853, United States; orcid.org/0000-0002-7396-2476

Complete contact information is available at: https://pubs.acs.org/10.1021/acs.langmuir.2c03005

Notes

The authors declare no competing financial interest.

ACKNOWLEDGMENTS

The project was sponsored by the Department of the Navy, Office of Naval Research, under ONR award N00014-23-1-2189. This work made use of the Cornell Center for Materials Research Shared Facilities which are supported through the NSF MRSEC program (DMR-1719875).

NOMENCLATURE

FTIR, Fourier transform infrared; XPS, X-ray photoelectron spectroscopy; S_N2 , second-order nucleophilic substitution; AR-XPS, angle-resolved X-ray photoelectron spectroscopy; HFBA, 2,2,3,4,4,4-hexafluorobutyl acrylate; PFOA, 1H,1H,2H,2H-perfluorooctyl acrylate; DEGDVE, di(ethylene glycol) divinyl ether; PFA, perfluorinated acid; NaOH, sodium hydroxide; TBPO, di-*tert*-butyl peroxide; TCVS, trichlorovinyl silane; CVD, chemical vapor deposition; iCVD, initiated chemical vapor deposition; IMFP, inelastic mean free path; FTIR-ATR, Fourier transform infrared with attenuated total reflectance

■ REFERENCES

- (1) Ulbricht, U. Advanced Functional Polymer Membranes. *Polymer* **2006**, 47, 2217–2262.
- (2) Qing, W.; Liu, F.; Yao, H.; Sun, S.; Chen, C.; Zhang, W. Functional Catalytic Membrane Development: A Review of Catalyst Coating Techniques. *Adv. Colloid Interface Sci.* **2020**, 282, 102207.
- (3) Guo, Y.; Liu, W.; Yan, Z. Synthesis and Characterization of Fluorinated Acrylic Polymer and the Properties of Epoxy Thermosets Modified With It. *J. Macromol. Sci. A* **2015**, *52*, 838–846.
- (4) Castelvetro, V.; Aglietto, M.; Ciardelli, F.; Chiantore, O.; Lazzari, M.; Toniolo, L. Structure Control, Coating Properties, and Durability of Fluorinated Acrylic-Based Polymers. *J. Coat. Technol.* **2002**, *74*, 57–66
- (5) Karaman, M.; Yenice, E. Plasma Enhanced Chemical Vapor Deposition of Poly(2,2,3,4,4,4-Hexafluorobutyl Acrylate) Thin Films. *Chem. Vap. Depos.* **2015**, *21*, 188–195.
- (6) Şimşek, B.; Karaman, M. Initiated Chemical Vapor Deposition of Poly(Hexafluorobutyl Acrylate) Thin Films for Superhydrophobic Surface Modification of Nanostructured Textile Surfaces. *J. Coat. Technol. Res.* **2019**, *17*, 381–391.
- (7) Buck, R. C.; Franklin, J.; Berger, U.; Conder, J. M.; Cousins, I. T.; de Voogt, P.; Jensen, A. A.; Kannan, K.; Mabury, S. A.; van Leeuwen, S. P. Perfluoroalkyl and Polyfluoroalkyl Substances in the

- Environment: Terminology, Classification, and Origins. *Integr. Environ. Assess. Manag.* **2011**, *7*, 513–541.
- (8) van Zoelen, W.; Buss, H. G.; Ellebracht, N. C.; Lynd, N. A.; Fischer, D. A.; Finlay, J.; Hill, S.; Callow, M. E.; Callow, J. A.; Kramer, E. J.; Zuckermann, R. N.; Segalman, R. A. Sequence of Hydrophobic and Hydrophilic Residues in Amphiphilic Polymer Coatings Affects Surface Structure and Marine Antifouling/Fouling Release Properties. *ACS Macro Lett.* **2014**, *3*, 364–368.
- (9) Mohammadi Ghaleni, M.; Tavakoli, E.; Bavarian, M.; Nejati, S. Fabricating Janus Membranes via Physicochemical Selective Chemical Vapor Deposition. *AIChE J.* **2020**, *66*, No. e17019.
- (10) Cheng, C.; Gupta, M. Solvent-Free Synthesis of Selectively Wetting Multilayer and Janus Membranes. *Adv. Mater. Interfaces* **2020**, *7*, 2001103.
- (11) Tufani, A.; Ozaydin Ince, G. Protein Gating by Vapor Deposited Janus Membranes. J. Membr. Sci. 2019, 575, 126–134.
- (12) You, J. B.; Yoo, Y.; Oh, M. S.; Im, S. G. Simple and Reliable Method to Incorporate the Janus Property onto Arbitrary Porous Substrates. ACS Appl. Mater. Interfaces 2014, 6, 4005–4010.
- (13) Wu, C.-Y.; Hsieh, H.-P.; Chen, S.-T.; Liu, T.-Y.; Chen, H.-Y. Fabrication of Functional Polymer Structures through Bottom-Up Selective Vapor Deposition from Bottom-Up Conductive Templates. *Langmuir* **2018**, *34*, 4651–4657.
- (14) Im, S. G.; Kim, B.-S.; Tenhaeff, W. E.; Hammond, P. T.; Gleason, K. K.A Directly Patternable Click-Active Polymer Film via Initiated Chemical Vapor Deposition (ICVD). *Proceedings of the Fifth International Conference on Hot-Wire CVD Cat-CVD Process*, 2009; Vol. 517 (12), pp 3606–3611.
- (15) Wu, C.-Y.; Hsieh, H.-P.; Chen, S.-T.; Liu, T.-Y.; Chen, H.-Y. Fabrication of Functional Polymer Structures through Bottom-Up Selective Vapor Deposition from Bottom-Up Conductive Templates. *Langmuir* **2018**, *34*, 4651–4657.
- (16) Elkasabi, Y.; Lahann, J. Vapor-Based Polymer Gradients. *Macromol. Rapid Commun.* **2009**, *30*, 57–63.
- (17) Elkasabi, Y. M.; Lahann, J.; Krebsbach, P. H. Cellular Transduction Gradients via Vapor-Deposited Polymer Coatings. *Biomaterials* **2011**, *32*, 1809–1815.
- (18) Ross, A. M.; Lahann, J. Surface Engineering the Cellular Microenvironment via Patterning and Gradients. *J. Polym. Sci. B* **2013**, *51*, *775*–794.
- (19) Söz, Ç. K.; Trosien, S.; Biesalski, M. Janus Interface Materials: A Critical Review and Comparative Study. *ACS Mater. Lett.* **2020**, *2*, 336–357.
- (20) Chen, Y.; Lu, K.-J.; Japip, S.; Chung, T.-S. Can Composite Janus Membranes with an Ultrathin Dense Hydrophilic Layer Resist Wetting in Membrane Distillation? *Environ. Sci. Technol.* **2020**, *54*, 12713–12722.
- (21) Gauthier, M. A.; Gibson, M. I.; Klok, H.-A. Synthesis of Functional Polymers by Post-Polymerization Modification. *Angew. Chem.* **2008**, 48, 48–58.
- (22) Jagur-Grodzinski, J.Surface Modification Procedures. *Heterogeneous Modification of Polymers*; John Wiley & Sons Ltd.: West Sussex, England, 1997; p 203.
- (23) Tenhaeff, W. E.Reactive and Stimuli-Responsive Polymer Thin Films. *CVD Polymers: Fabrication of Organic Surfaces and Devices*; Wiley-VCH Verlag GmbH & Co.: Weinheim, Germany, 2015; pp 173–198.
- (24) Deng, X.; Cheng, K. C. K.; Lahann, J.Multifunctional Reactive Polymer Coatings. *CVD Polymers: Fabrication of Organic Surfaces and Devices*; Wiley-VCH Verlag GmbH & Co.: Weinheim, Germany, 2015; pp 199–218.
- (25) O'Shaughnessy, W. S.; Marí-Buyé, N.; Borrós, S.; Gleason, K. K. Initiated Chemical Vapor Deposition of a Surface-Modifiable Copolymer for Covalent Attachment and Patterning of Nucleophilic Ligands. *Macromol. Rapid Commun.* **2007**, 28, 1877–1882.
- (26) Montero, L.; Baxamusa, S. H.; Borros, S.; Gleason, K. K. Thin Hydrogel Films With Nanoconfined Surface Reactivity by Photo-initiated Chemical Vapor Deposition. *Chem. Mater.* **2009**, *21*, 399–403.

- (27) Marí-Buyé, N.; O'Shaughnessy, S.; Colominas, C.; Semino, C. E.; Gleason, K. K.; Borrós, S. Functionalized, Swellable Hydrogel Layers as a Platform for Cell Studies. *Adv. Funct. Mater.* **2009**, *19*, 1276–1286.
- (28) Deng, X.; Eyster, T. W.; Elkasabi, Y.; Lahann, J. Bio-Orthogonal Polymer Coatings for Co-Presentation of Biomolecules. *Macromol. Rapid Commun.* **2012**, 33, 640–645.
- (29) Xu, J.; Gleason, K. K. Conformal, Amine-Functionalized Thin Films by Initiated Chemical Vapor Deposition (ICVD) for Hydrolytically Stable Microfluidic Devices. *Chem. Mater.* **2010**, 22, 1732–1738
- (30) Lau, K. K. S.; Gleason, K. K. Particle Functionalization and Encapsulation by Initiated Chemical Vapor Deposition (ICVD). *Surf. Coat. Technol.* **2007**, 201, 9189–9194.
- (31) Im, S. G.; Bong, K. W.; Lee, C.-H.; Doyle, P. S.; Gleason, K. K. A Conformal Nano-Adhesive via Initiated Chemical Vapor Deposition for Microfluidic Devices. *Lab Chip* **2009**, *9*, 411–416.
- (32) Lahann, J.; Balcells, M.; Lu, H.; Rodon, T.; Jensen, K. F.; Langer, R. Reactive Polymer Coatings: A First Step toward Surface Engineering of Microfluidic Devices. *Anal. Chem.* **2003**, *75*, 2117–2122.
- (33) Arora, W. J.; Tenhaeff, W. E.; Gleason, K. K.; Barbastathis, G. Integration of Reactive Polymeric Nanofilms Into a Low-Power Electromechanical Switch for Selective Chemical Sensing. *J. Microelectromech. Syst.* **2009**, *18*, 97–102.
- (34) Tenhaeff, W. E.; Gleason, K. K. Surface-Tethered pH-Responsive Hydrogel Thin Films as Size-Selective Layers on Nanoporous Asymmetric Membranes. *Chem. Mater.* **2009**, 21, 4323–4331.
- (35) Lahann, J.; Balcells, M.; Rodon, T.; Lee, J.; Choi, I. S.; Jensen, K. F.; Langer, R. Reactive Polymer Coatings: A Platform for Patterning Proteins and Mammalian Cells onto a Broad Range of Materials. *Langmuir* **2002**, *18*, 3632–3638.
- (36) Chen, H.-Y.; Elkasabi, Y.; Lahann, J. Surface Modification of Confined Microgeometries via Vapor-Deposited Polymer Coatings. *J. Am. Chem. Soc.* **2006**, *128*, 374–380.
- (37) Elkasabi, Y.; Chen, H.-Y.; Lahann, J. Multipotent Polymer Coatings Based on Chemical Vapor Deposition Copolymerization. *Adv. Mater.* **2006**, *18*, 1521–1526.
- (38) Tsai, M.-Y.; Lin, C.-Y.; Huang, C.-H.; Gu, J.-A.; Huang, S.-T.; Yu, J.; Chen, H.-Y. Vapor-Based Synthesis of Maleimide-Functionalized Coating for Biointerface Engineering. *Chem. Commun.* **2012**, 48, 10969–10971.
- (39) Wu, J.-T.; Huang, C.-H.; Liang, W.-C.; Wu, Y.-L.; Yu, J.; Chen, H.-Y. Reactive Polymer Coatings: A General Route to Thiol-Ene and Thiol-Yne Click Reactions. *Macromol. Rapid Commun.* **2012**, *33*, 922–927.
- (40) Im, S. G.; Bong, K. W.; Kim, B.-S.; Baxamusa, S. H.; Hammond, P. T.; Doyle, P. S.; Gleason, K. K. Patterning Nanodomains with Orthogonal Functionalities: Solventless Synthesis of Self-Sorting Surfaces. J. Am. Chem. Soc. 2008, 130, 14424–14425.
- (41) Shafi, H. Z.; Wang, M.; Gleason, K. K.; Khan, Z. Synthesis of Surface-Anchored Stable Zwitterionic Films for Inhibition of Biofouling. *Mater. Chem. Phys.* **2020**, 239, 121971.
- (42) Nandivada, H.; Chen, H.-Y.; Bondarenko, L.; Lahann, J. Reactive Polymer Coatings that "Click". *Angew. Chem., Int. Ed.* **2006**, 45, 3360–3363.
- (43) Chen, G.; Gupta, M.; Chan, K.; Gleason, K. K. Initiated Chemical Vapor Deposition of Poly(Furfuryl Methacrylate). *Macromol. Rapid Commun.* **2007**, 28, 2205–2209.
- (44) Sartipek, F.; Karaman, M. Initiated CVD of Tertiary Amine-Containing Glycidyl Methacrylate Copolymer Thin Films for Low Temperature Aqueous Chemical Functionalization. *Chem. Vap. Depos.* **2014**, *20*, 373–379.
- (45) Yagüe, J. L.CVD Fluoropolymers. CVD Polymers; John Wiley & Sons, Ltd., 2015; pp 219-232.
- (46) Asatekin, A.; Gleason, K. K. Polymeric Nanopore Membranes for Hydrophobicity-Based Separations by Conformal Initiated Chemical Vapor Deposition. *Nano Lett.* **2011**, *11*, 677–686.

- (47) Cheng, Y.; Khlyustova, A.; Chen, P.; Yang, R. Kinetics of All-Dry Free Radical Polymerization under Nanoconfinement. *Macromolecules* **2020**, *53*, 10699–10710.
- (48) Asatekin, A.; Barr, M. C.; Baxamusa, S. H.; Lau, K. K. S.; Tenhaeff, W.; Xu, J.; Gleason, K. K. Designing Polymer Surfaces via Vapor Deposition. *Mater. Today* **2010**, *13*, 26–33.
- (49) Baxamusa, S. H.; Im, S. G.; Gleason, K. K. Initiated and Oxidative Chemical Vapor Deposition: A Scalable Method for Conformal and Functional Polymer Films on Real Substrates. *Phys. Chem. Chem. Phys.* **2009**, *11*, 5227–5240.
- (50) Yu, S. J.; Pak, K.; Kwak, M. J.; Joo, M.; Kim, B. J.; Oh, M. S.; Baek, J.; Park, H.; Choi, G.; Kim, D. H.; Choi, J.; Choi, Y.; Shin, J.; Moon, H.; Lee, E.; Im, S. G. Initiated Chemical Vapor Deposition: A Versatile Tool for Various Device Applications. *Adv. Eng. Mater.* **2018**, 20, 1700622.
- (51) Burwell, R. L. The Cleavage of Ethers. Chem. Rev. 1954, 54, 615-685.
- (52) Van Guyse, J. F. R.; Verjans, J.; Vandewalle, S.; De Bruycker, K.; Du Prez, F. E.; Hoogenboom, H. Full and Partial Amidation of Poly(Methyl Acrylate) as Basis for Functional Polyacrylamide (Co)Polymers. *Macromolecules* **2019**, *52*, 5102–5109.
- (53) Lamch, Ł.; Ronka, S.; Moszyńska, I.; Warszyński, P.; Wilk, K. A. Hydrophobically Functionalized Poly(Acrylic Acid) Comprising the Ester-Type Labile Spacer: Synthesis and Self-Organization in Water. *Polymers* **2020**, *12*, 1185.
- (\$4) Bensacia, N.; Moulay, S. Functionalization of Polyacrylic Acid with Tetrahydroxybenzene via a Homolytic Pathway: Application to Metallic Adsorption. *Int. J. Polym. Mater. Polym. Biomater.* **2012**, *61*, 699–722.
- (55) Tanuma, S.; Powell, C. J.; Penn, D. R. Calculations of Electron Inelastic Mean Free Paths. V. Data for 14 Organic Compounds over the 50–2000 eV Range. *Surf. Interface Anal.* **1994**, *21*, 165–176.
- (56) Hind, A. R.; Bhargava, S. K.; McKinnon, A. At the Solid/Liquid Interface: FTIR/ATR—the Tool of Choice. *Adv. Colloid Interface Sci.* **2001**, 93, 91–114.
- (57) Krishnaswamy, R. K.; Janzen, J. Exploiting Refractometry to Estimate the Density of Polyethylene: The Lorentz–Lorenz Approach Re-Visited. *Polym. Test.* **2005**, *24*, 762–765.
- (58) Refraction and Refractive Index. Lange's Handbook of Chemistry; Speight, J. G., Ed.; McGraw-Hill Education: New York, 2017.
- (59) Poly(2,2,3,4,4,4-Hexafluorobutyl Acrylate) SDS, 2020. https://sigmaaldrich.com/US/en/sds/aldrich/630160.
- (60) Yılmaz, K.; Gürsoy, M.; Karaman, M. Vapor Deposition of Transparent Antifogging Polymeric Nanocoatings. *Langmuir* **2021**, 37, 1941–1947.
- (61) Brinker, C. J. Hydrolysis and Condensation of Silicates: Effects on Structure. *J. Non-Cryst. Solids* **1988**, *100*, 31–50.
- (62) Singh, M. P.; Keister, H. K.; Matisons, J. G.; Pan, Y.; Zazyczny, J.; Arkles, B. Dipodal Silanes: Important Tool for Surface Modification to Improve Durability. *MRS Online Proc. Libr.* **2014**, 1648, 201.
- (63) Hofmann, S.Optimizing Measured Signal Intensity: Emission Angle, Incidence Angle and Surface Roughness. Auger- and X-ray Photoelectron Spectroscopy in Materials Science; Springer Series in Surface Sciences; Springer: Berlin, 2013; Vol. 49, pp 205–257.
- (64) Yang, C.; Xing, X.; Li, Z.; Zhang, S. A Comprehensive Review on Water Diffusion in Polymers Focusing on the Polymer-Metal Interface Combination. *Polymers* **2020**, *12*, 138.
- (65) Evans, S. Correction for the Effects of Adventitious Carbon Overlayers in Quantitative XPS Analysis. *Surf. Interface Anal.* **1997**, 25, 9242–9930.
- (66) Beamson, G.; Alexander, M. R. Angle-Resolved XPS of Fluorinated and Semi-Fluorinated Side-Chain Polymers. *Surf. Interface Anal.* **2004**, *36*, 323–333.
- (67) Sharma, R. C.; Sharma, M. M. Kinetics of Alkaline Hydrolysis of Esters. II. Unsaturated Esters and Oxalic Esters. *Bull. Chem. Soc. Jpn.* **1970**, 43, 642–645.

- (68) Mallik, K. L.; Das, M. N. Alkaline Hydrolysis of Acrylic and Methacrylic Esters in 60% Aqueous Ethanol. *Naturwissenschaften* 1964, 51, 37.
- (69) Kwok, D. Y.; Neumann, A. W. Contact Angle Measurement and Contact Angle Interpretation. *Adv. Colloid Interface Sci.* **1999**, *81*, 167–249.
- (70) Liu, A.; Goktekin, E.; Gleason, K. K. Cross-Linking and Ultrathin Grafted Gradation of Fluorinated Polymers Synthesized via Initiated Chemical Vapor Deposition To Prevent Surface Reconstruction. *Langmuir* **2014**, *30*, 14189–14194.
- (71) Raj, R.; Enright, R.; Zhu, Y.; Adera, S.; Wang, E. N. Unified Model for Contact Angle Hysteresis on Heterogeneous and Superhydrophobic Surfaces. *Langmuir* **2012**, *28*, 15777–15788.
- (72) Xiao, C.; Zhang, S.-L. Mechanism for Acetic Acid-Catalyzed Ester Aminolysis. *Chin. Chem. Lett.* **2018**, *29*, 1233–1236.

□ Recommended by ACS

Network Degradation Assessed by Evolved Gas Analysis-Mass Spectrometry Combined with Principal Component Analysis (EGA-MS-PCA): A Case of Therm...

Takato Ishida, Ryota Watanabe, et al.

JANUARY 18, 2023 MACROMOLECULES

READ 🗹

Effective Removal and Resource Recovery for Heavy Metal-Organic Complex-Polluted Water via an Integrated Decomplexation-Degradation-Immobilization Pathway

Shangying Li, Hong Chen, et al.

JANUARY 20, 2023

ACS ES&T WATER

READ 🗹

Space Charge Contributions to the Dielectric Response and Breakdown Strength of High-Temperature Poly(ether imide)/Polyimide Blends

Vida Jurečič, Vid Bobnar, et al.

JANUARY 13, 2023 MACROMOLECULES

READ 🗹

Demystifying the Role of Surfactant in Tailoring Polyamide Morphology for Enhanced Reverse Osmosis Performance: Mechanistic Insights and Environmental Implications

Qimao Gan, Chuyang Y. Tang, et al.

JANUARY 18, 2023

ENVIRONMENTAL SCIENCE & TECHNOLOGY

READ 🗹

Get More Suggestions >